Nonlinear Dynamics and Neuroscience

Article DOI: 10.18500/0869-6632-003210

Neural network as an indicator of connectivity in an ensemble of chaotic systems

A. V. Shabunin

Saratov State University, Russia
E-mail: ✉shabuninav@info.sgu.ru

Received 12.12.2025, accepted 4.01.2026, available online 27.01.2026, published 31.03.2026

Abstract. The *purpose* of this work is development and research of an algorithm for determining the structure of coupling of an ensemble of chaotic systems under conditions of external noise. *The method* is based on the Granger causality approach and the use of artificial direct propagation neural networks trained with regularization. *Results.* We have developed a method to identify the structure of couplings of a network of chaotic maps, which is based on the Granger causality principle and artificial neural networks. It represents a modification of the previously proposed algorithm and allows us to find the connectivity of the ensemble as a whole by a single pass of the network training. The algorithm has shown its effectiveness for an example of a small ensemble of non-identical maps with linear couplings. It keeps to work at presences of weak external noise, although the accuracy of the method deteriorates with the noise intensity. *Discussion.* The method has demonstrated its effectiveness for simple mathematical models, including in the presence of noise. However, its effectiveness at larger noise intensity requires additional statistical processing methods. It is also interesting to consider how it works for other types of couplings.

Keywords: dynamical chaos, artificial neural networks, ensembles of maps, couplings structure identification.

For citation: Shabunin AV. Neural network as an indicator of connectivity in an ensemble of chaotic systems. Izvestiya VUZ. Applied Nonlinear Dynamics. 2026;34(2):331–344. DOI: 10.18500/0869-6632-003210

Introduction

In [1, 2], an algorithm for determining the structure of couplings in an ensemble of chaotic maps based on the use of an artificial neural network (ANN) trained with a teacher was considered. This task is called *determining the connectivity*. To solve this problem, various methods are used to analyze the signals generated by the subsystems that make up the ensemble, one of which is the calculation of *Granger causality (GC)* [3, 4]. This method is based on the assumption that if system A affects system B, then taking into account the state of A should improve the prediction of $B's$ behavior. This improvement is reflected in the reduction of the mean squared error of the prediction $\varepsilon = \sqrt{\left\langle \left|\overline{B} - B\right|^2 \right\rangle}$, where $\overline{B}$ is the predicted value. Accordingly, the degree of influence of A on B can be estimated by the reduction of ε due to the inclusion of information about A: $PI = \left(\varepsilon^2 - \varepsilon_A^2\right)/\varepsilon^2$ [5].

Using GC requires the construction of an appropriate predictor filter[1], which is a complex and ambiguous task in itself. Therefore, there are many methods for determining connectivity applied to

[1] A predictor filter is an $N \times M$ network that uses N previous signal samples to predict M subsequent samples.

various natural [6–12] and model [13–15] systems. The variety of approaches used indicates the lack of a single effective algorithm for determining connectivity, so the task of developing such an algorithm remains relevant.

One of the tools for predicting the behavior of systems based on the time series they generate is an artificial neural network of direct propagation [16,17]. The ability of ANN to solve such problems is well known [18–21]. In addition, the ANN has its own network structure, which, changing during training, can, under certain conditions, adapt to the structure of the ensemble's couplings and thereby identify the latter. To ensure this adjustment, it is necessary to use the *regularization training* procedure [22]. The regularization method was first proposed by A. N. Tihonov [23] and has been widely used in optimization problems. Its essence lies in the introduction of the so-called «complexity penalty» of the network, which provides «zeroing» unnecessary synaptic coefficients. This removes the «superfluous» couplings and leaves only those that are necessary for correct prediction.

In [1], it was proposed to use a regularization training procedure to identify diffusion couplings between N identical one-dimensional chaotic maps. To do this, the ANN was consistently trained to predict the dynamics of each of the N maps individually, using signals from all network nodes as input data. Based on the results of the training, it was determined which nodes of the ensemble are associated with the map, whose dynamics are predicted. Accordingly, to determine the entire structure of the ensemble's couplings, it was necessary to conduct N separate training procedures. As it turned out, this method is redundant. In this paper, we propose a modified algorithm that allows us to identify a complete picture of the couplings in the ensemble as a result of training the ANN to predict its dynamics as a whole. In addition, we have moved away from the previously used constraints on the identity of subsystems and on the diffusion type of couplings between the elements of the ensemble.

1. Problem statement

Consider a network of N one-dimensional chaotic subsystems with discrete time, interconnected by individual couplings:

$$x_i(n+1) = f_i(x_i(n)) + \sum_{\substack{j=1 \\ j\neq i}}^{N} \gamma_{ij}(g_{ij}x_j(n)), \quad i = 1, ..., N. \tag{1}$$

Here $x_i(n)$ is a real dynamic variable describing the state of the ith subsystem at time n, f_i is a function defining its individual dynamics, γ_{ij} is a coupling function describing the effect of the j node on the i node, g_{ij} is the corresponding coupling coefficient.

We will assume that all couplings are passive, that is, they do not contain their own signal sources. Therefore, all $\gamma_{ij}(0) = 0$. In addition, let us assume that the functions γ_{ij} do not take extreme or stationary values at zero, and the dynamics of ensemble (1) is finite. Then with weak couplings (that is, with $g_{ij} \ll 1/a_j$, where $a_j = \max|x_j|$) they can be linearized in the vicinity of zero: $\gamma_{ij}(x) \simeq g_{ij}x$. Subject to the structural stability of system (1) such coarsening should not significantly affect the steady state oscillatory modes of the ensemble and, accordingly, the operation of the method for determining its connectivity. Therefore, further we will consider only linear couplings.

In this study, logistic maps are used as the subsystems: $f_i = \alpha_i x_i(1 - x_i)$, which are in developed chaotic mode; the latter is provided by the appropriate choice of parameters α_i. The coupling functions between the maps are assumed to be linear: $\gamma_{ij} = g_{ij}x_j$. Taking into account the above, system (1) takes the form

$$x_i(n+1) = \alpha_i x_i(n)(1 - x_i(n)) + \sum_{j=1}^{N} g_{ij}x_j(n), \quad i = 1, ..., N, \tag{2}$$

where all $g_{ii} = 0$. It is convenient to rewrite it in matrix-vector form:

$$\mathbf{x}(n+1) = \mathbf{f}(\mathbf{x}(n)) + \hat{G}\mathbf{x}(n), \tag{3}$$

where $\mathbf{x} = [x_1, x_2, \ldots, x_N]^T$ is a vector column of variables (index T means transpose), $\hat{G}$ is the matrix of ensemble couplings ($G_{ij} = g_{ij}$), $\mathbf{f}(\mathbf{x}) = [f_1(x_1), f_2(x_2), \ldots, f_N(x_N)]^T$ is the vector function of maps.

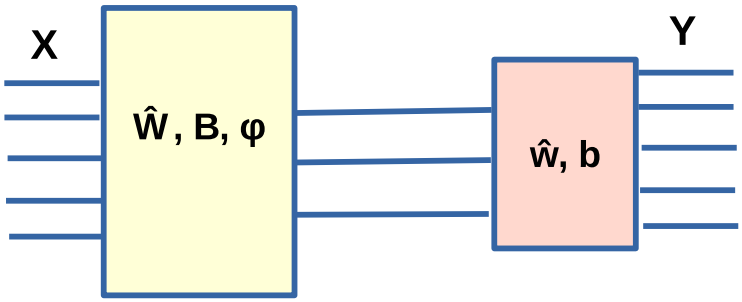

Fig. 1. The scheme of a two-layer neural network: $\mathbf{X}$ and $\mathbf{Y}$ are vectors of input and output signals, $\hat{W}$ and $\hat{w}$ are matrices of synaptic coefficients of neurons of the first and the second layers, respectively, while vectors $\mathbf{B}$ and $\mathbf{b}$ represent the values of their offsets, $\boldsymbol{\varphi}(x) = \mathrm{th}(x)$ is the activation function of the neurons of the first layer; the second layer is linear

The estimate of $\hat{G}$ based on the observed signal $\mathbf{x}\,(n)$ is a solution to the problem of determining the connectivity of ensemble (2).

The algorithm for determining the structure of couplings is based on the use of ANN of forward propagation, trained with a teacher [16]. Such neural networks successfully perform the tasks of predicting the future dynamics of a system based on its previous data. To do this, during the training process, the ANN rebuilds the couplings between neurons. In this paper, we will try to organize this process in such a way as to adapt the couplings of the neural network to the structure of the couplings of ensemble (2).

To solve this problem, we use a two-layer ANN, the structure of which is shown in Fig. 1. The equation of such a network has the form

$$\mathbf{Y} = \hat{w}\boldsymbol{\varphi}\left(\hat{W}\mathbf{X} + \mathbf{B}\right) + \mathbf{b}, \tag{4}$$

where $\mathbf{X}$ and $\mathbf{Y}$ are the N-dimensional vectors of the input and output signals, respectively. The values of all N maps at the current time are used as $\mathbf{X}$: $\mathbf{X}\,(n) = [\tilde{x}_1(n), \tilde{x}_2(n), ..., \tilde{x}_N(n)]^T$. To exclude the influence of factors such as the amplitude and offset of the signals, they are pre-centered and normalized by amplitude: $x_i \to \tilde{x}_i$. The dimension of the hidden layer (m) is not directly related to the dimension of the ensemble, but is determined by the complexity of the task. Recommendations for selecting this parameter are listed in [16]. This study uses $m = 10$. The hyperbolic tangent is chosen as the activation function of $\varphi(x)$, since it vanishes with a zero argument and, moreover, is the standard choice for direct propagation ANN.

2. The training algorithm of ANN for evaluating connectivity

2.1. General description. During training with a teacher, network (4) changes the values of synaptic coefficients and offset vectors so as to approximate the right-hand sides of equations (2) with a given accuracy. The possibility of this with a sufficient amount of training data and hidden layer neurons is guaranteed by the Kolmogorov–Arnold theorem [24,25]. Let us consider how the obtained values of the coefficients of the matrices $\hat{W}$ and $\hat{w}$ are related to the structure of ensemble equations (3), namely with the couplings matrix $\hat{G}$. To do this, write down the coupling lth components of the ANN output signal (that is, $Y_l(n)$) with all N current values of $\tilde{x}_i(n)$ $(i = 1, ..., N)$:

$$Y_l(n) = b_l + \sum_{k=1}^{m} w_{lk}\mathrm{th}\left(B_k + \sum_{i=1}^{N} W_{ki}\tilde{x}_i(n)\right). \tag{5}$$

If the value of the hyperbolic tangent argument is not very large, it can be approximately replaced by a linear function:

$$Y_l(n) \simeq b_l + \sum_{k=1}^{m} w_{lk}B_k + \sum_{k=1}^{m} w_{lk}\sum_{i=1}^{N} W_{ki}\tilde{x}_i(n). \tag{6}$$

Replacing the order of summation in the last term, we rewrite this expression as

$$Y_l(n) \simeq b_l + \sum_{k=1}^{m} w_{lk} B_k + \sum_{i=1}^{N} C_{li} \tilde{x}_i(n), \tag{7}$$

where $C_{li} = \sum_k w_{lk} W_{ki}$ is the matrix coefficient of the product $\hat{w}\hat{W}$. As can be seen from formula (7), this coefficient characterizes the effect of the ith map on the lth output of the neural network, that is, it indicates the coupling between them. The latter is a prediction of the value of $\tilde{x}_l(n+1)$. Thus, the $N \times N$ matrix $\hat{C} = \hat{w}\hat{W}$ can be used to diagnose the coupling matrix $\hat{G}$.

As a rule, the average square of the prediction errors is chosen as the objective function for training ANN to predict time series:

$$\Phi = \frac{1}{KN} \sum_{n=0}^{K-1} \sum_{l=1}^{N} \left(Y_l(n) - D_l(n) \right)^2, \tag{8}$$

where K is the number of training vectors, $D_l(n)$ is the predicted value of the lth map; in our case, it is the following in time: $D_l(n) = \tilde{x}_l(n+1)$. The purpose of the training is to reach the Φ point of the global minimum. Will the value of the ANN coefficients at the minimum point Φ correspond to the structure of the couplings of the ensemble whose dynamics is predicted? Obviously, such a correspondence is not necessary: a minimum of Φ can also be achieved with excessive values of couplings between neurons, since in formula (8) the latter are not limited in any way. In order to encourage ANN to «limit» couplings during training, it was proposed in work of [22] to use a regularization procedure consisting in the introduction of «penalty» for the values of synaptic coefficients:

$$P = r \left(\sum_{i=1}^{m} \sum_{j=1}^{N} W_{ij}^2 + \sum_{i=1}^{N} \sum_{j=1}^{m} w_{ij}^2 \right), \tag{9}$$

which represents the rth part of the total sum of their squares. The parameter $r \geqslant 0$ is called *regularization coefficient* (RC). As a result, the modified objective function takes the form

$$\Psi = \Phi + P. \tag{10}$$

This form of objective function characterizes the ability to predict the dynamics of an ensemble of map with minimal couplings between neurons of ANN. At the same time, couplings that are unnecessary for successful prediction are suppressed. After their «zeroing» the obtained values of the coefficients C_{ij} will make it possible to diagnose the structure of the couplings between the nodes of the ensemble under study.

Thus, the values of the off-diagonal coefficients of the matrix $\hat{C}$ obtained at the end of the regularization training procedure are used to diagnose the matrix $\hat{G}$. For this purpose, we will also apply the procedure of their normalization by diagonal coefficients: $S_{ij} = C_{ij}/C_{ii}$. The value of S_{ij} will be called the *influence coefficient* of jth nodes on the ith, and the matrix built from them $\hat{S}$ is the *influence matrix*. The latter is used to determine the qualitative form of the coupling matrix $\hat{G}$.

Thus, the proposed method for diagnosing the connectivity of an ensemble of maps is as follows.

1. An ANN is being created, the structure of which is shown in Fig. 1, with input and output dimensions equal to the number of ensemble elements N, and the number of hidden layer neurons is $m = 10$.
2. Network coefficients are initialized with random values.
3. To train an ANN, a training set is formed from $K = 1000$ vectors $\{\mathbf{X}(n)\}_{n=0}^{K-1}$, each of which represents a map of the entire ensemble at the nth moment in time: $\mathbf{X}(n) = \tilde{\mathbf{x}}(n)$, and set of target values $\{\mathbf{D}(n)\}_{n=0}^{K-1}$, which are taken as subsequent values of the same quantities: $\mathbf{D}(n) = \tilde{\mathbf{x}}(n+1)$.
4. The network is trained based on objective function (10). A Quasi-Newton algorithm is used for training, which refers to second-order methods and has faster convergence compared to gradient methods. The duration of the training is set at 1000 epochs.
5. The influence matrix $\hat{S}$ is calculated to identify the couplings.

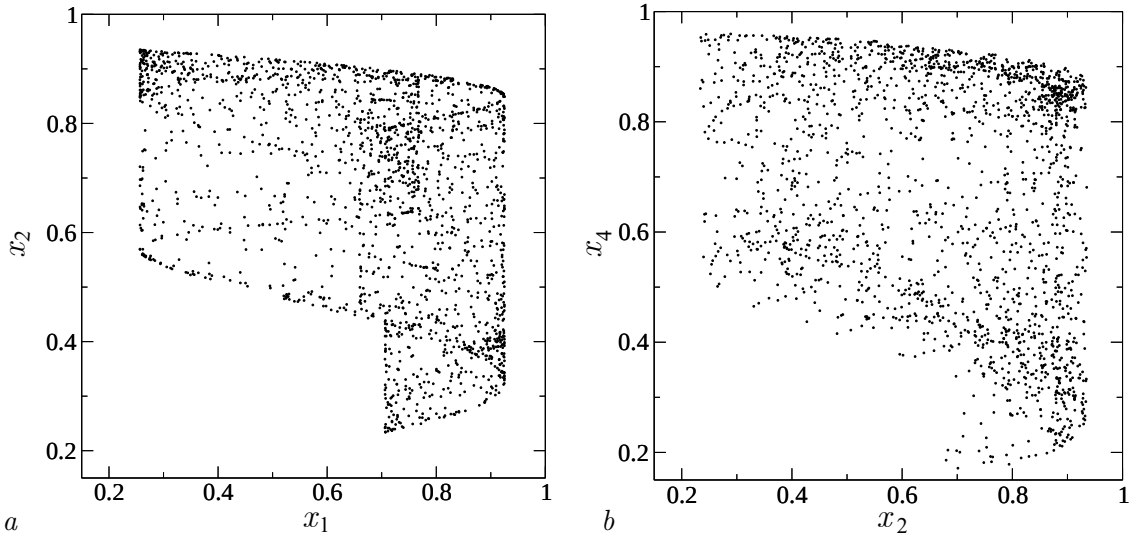

Fig. 2. Projections of phase portraits of system (2) on $x_1 - x_2$ (a) and $x_2 - x_4$ (b) planes at the chosen parameters

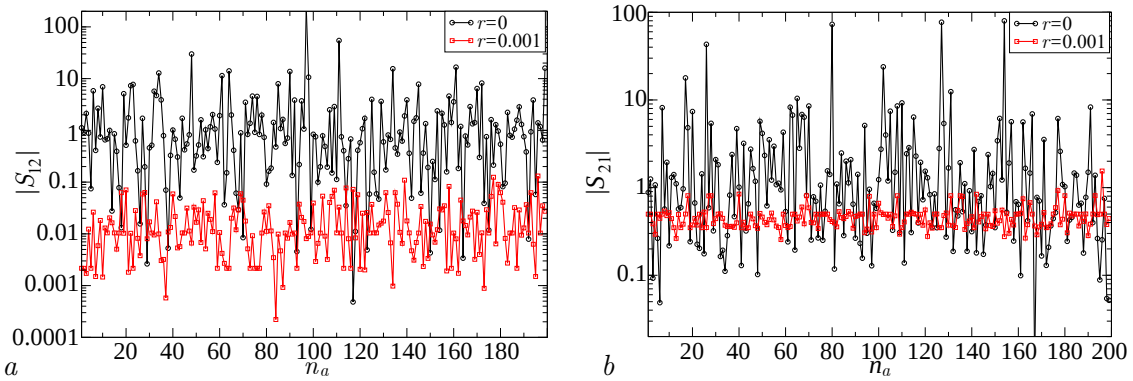

Fig. 3. The dependence of the modules of influence coefficients $|S_{12}|$ (a) and $|S_{21}|$ (b) on the number of training attempts n_a for different values of regularization parameter r

Note that since the training method is based on random initial values of the ANN coefficients, and the Ψ function has many local minima, the training process will produce random results[2], the processing of which requires the use of statistical methods.

2.2. Numerical studies of the algorithm. To test the algorithm, we select ensemble (2) of four maps with parameters $\alpha = [3.7, 3, 2.6, 3.1]$ and the coupling matrix

$$G = 0.2 \begin{bmatrix} 0 & 0 & 0 & 0 \\ 1 & 0 & 0 & 0 \\ 1 & 1 & 0 & 0 \\ 0 & 1 & 0 & 0 \end{bmatrix}. \tag{11}$$

As can be seen from (11), unidirectional couplings of the same magnitude operate between the elements of the ensemble. In this case, the first node is completely autonomous, the second is affected by the signal from the first node, the third is affected by the signals of the first and second, and the fourth is affected only by the second. This coupling structure was chosen arbitrarily. Selected parameter values are not bifurcated, and their small change almost does not change the dynamics of the ensemble, which indicates

[2]Therefore, such methods are called *stochastic training*.

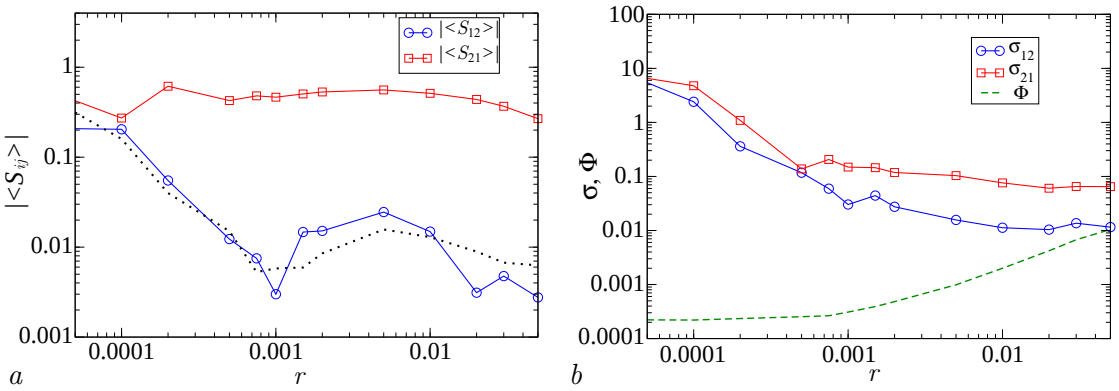

Fig. 4. The dependence of $|\langle S_{12}\rangle|$ and $|\langle S_{21}\rangle|$ (a), and the standard deviations σ_{12} and σ_{21} (b) from r; dashed line in subfigure (b) plots the graph of $\Phi(r)$

the robastness of the system. They correspond to the regime of developed non-synchronous chaos in all nodes, what can be seen from the projections of the phase portraits shown in Fig. 2.

Let us apply the methodology described in Section (2) to determine the connectivity in the considered ensemble. To do this, we will conduct a series of repeated attempts to train the ANN, starting with different initial values of the synaptic coefficients, and calculate the coefficients of the matrix $\hat{S}$ based on the results of each of them. As illustrative examples, we will use the values of the coefficients S_{12}, which corresponds to the «zero» coupling coefficient, and S_{21}, corresponding to the coupling value of 0.2.

First, we will train the ANN without regularization ($r = 0$). The training is successful, as seen from small value of the average square of prediction errors, which is $\sim 10^{-4}$ or less. However, the resulting coefficients of the matrix $\hat{S}$ do not have any repeatability, as evidenced by the graphs displaying the values $|S_{12}|$ (see Fig. 3, a) and $|S_{21}|$ (see Fig. 3, b), calculated based on the results of each training attempt[3]. It can be seen that both values exhibit random fluctuations of large amplitude, so that their standard deviations are $\sigma_{12} \simeq 18$ and $\sigma_{21} \simeq 10$ respectively. The latter significantly exceed the average values of the influence coefficients, which makes it impossible to draw a reliable conclusion about the corresponding coefficients of the matrix $\hat{G}$ based on them. The other coefficients S_{ij} behave similarly. At the same time, the value of the average square of prediction errors, which characterizes the quality of training, remains quite small: for most cases, it is less than 10^{-4} and only at certain points demonstrates outliers up to $\Phi \sim 0.001$.

Now we will apply the same technique for non-zero values of the regularization parameter. For example, let us choose a sufficiently small value: $r = 0.001$. The values of $|S_{12}|$ and $|S_{21}|$ obtained from training attempts are shown in the same subfigures 3, a and 3, b. As can be seen from the plots, regularization leads to significant stabilization of the values of the calculated coefficients, reducing the standard deviations to $\sigma_{12} \simeq 0.03$ and $\sigma_{21} \simeq 0.15$, respectively. At the same time, the average value is shifted «zero» coefficient $|S_{12}|$ up to the value of ~ 0.02.

Thus, the value of the regularization parameter significantly affects the measurement results of the matrix $\hat{S}$, making them more predictable. To analyze this effect, we will take measurements at different values of r and plot the dependence of the average values of the coefficients (Fig. 4, a) and their standard deviations (Fig. 4, b) from the regularization parameter.

As can be seen from Fig. 4, a, the average value of the «zero» coefficient S_{12} decreases rapidly to $|\langle S_{12}\rangle| \sim 0.01$ as r increases from zero to $r \simeq 0.0075$, after which it changes slightly in the vicinity of this value. The other «zero» coefficients behave in a similar way. In order not to clutter up the figure with a large number of similar curves, we have provided a graph of values averaged over all «zero» coefficients, which is displayed as a dotted line. It exhibits qualitatively similar behavior to $|\langle S_{12}\rangle|$. As for the average value of the coefficient S_{21}, like other «nonzero» coefficients, it weakly depends on r, demonstrating small

[3]The coefficients themselves can take both positive and negative values, however, since the graphs are plotted on a logarithmic scale, their modules are displayed on them.

oscillations in the vicinity of $|\langle S_{12}\rangle| \simeq 0.5$.

The repeatability of the measurement results S_{ij} can be characterized by the values of their standard deviations σ_{ij}. Dependencies σ_{12} and σ_{21} on r are shown in Fig. 4, *b*. Here we see a rapid decline at the initial stage: $r \in [0, 0.001]$, after which their values stabilize. The other coefficients σ_{ij} behave similarly.

Let us also consider the effect of r on the predictive ability of a trained neural network. Since «penalty» reduces the role of the mean squared error of prediction in evaluating the effectiveness of ANN, with an increase in r the value Φ should increase. This assumption is confirmed by the results of numerical experiments, the plot of which is shown in Fig. 4, *b* with a dashed line. The latter is a monotonically increasing function $\Phi(r)$. At the same time, at the initial stage, at $r < 0.001$, the increase of the mean squared error of prediction remains insignificant, and only at $r > 0.001$ does it significantly increases.

Thus, in order to obtain stable results of the coefficients of the influence matrix while maintaining the ability of the ANN to predict the dynamics of the ensemble, it is necessary to use the values of the regularization coefficient of the order of ~ 0.001. A further increase in r is impractical, since it has little effect on the magnitude and stability of the calculated data, significantly impairing the performance of the ANN as a predictor filter.

3. Calculation of the connectivity of the ensemble elements

In accordance with the recommendations received in the previous section, we will choose the value of $r = 0.001$, which we will use in further calculations. Let's consider the operation of an algorithm for determining connectivity during repeated attempts to train a network based on the same data, but from different initial conditions of the network itself. During the numerical simulation, 1000 such attempts were carried out, for each of which its own values of $\hat{S}$ were calculated. Based on the results obtained, the probability density functions $p_{ij} = p(S_{ij})$ were found. The plots for some of them are shown in Fig. 5.

For visual display, two coefficients were selected — S_{12} and S_{41} — from the category «zero», and two — S_{21} and S_{32} — from the category «nonzero». For the first one, the probability density is an almost symmetrical function with a sharp maximum near zero and a shape resembling a Gaussian curve. While moving away from zero, the value of the probability density decreases rapidly. The rest of the graphs shown in the figure relate to existing couplings. For them, probability densities are characterized by a complex shape with several maxima and a significant spread. Therefore, it is difficult to quantify the intensity of the coupling using them, one can only conclude about its existence.

To obtain an estimate of the coefficients of the influence matrix, we will use two estimation methods: the most likely values of the coefficients $\tilde{S}_{ij} = \arg(\max(p_{ij}))$ and average $\langle S_{ij}\rangle$. The estimate obtained for

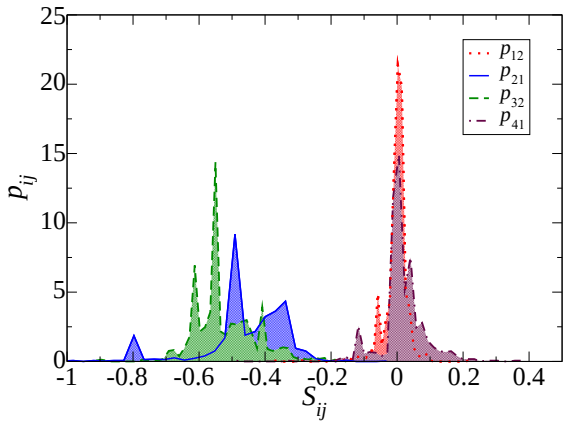

Fig. 5. Probability density of coefficients S_{12}, S_{21}, S_{32} and S_{41}, calculated from a series of 1000 training passes with regularization; $r = 0.001$ (color online)

the most probable values is presented in Table 1.

Table 1. Estimation of matrix $\hat{S}$ by maxima of distribution functions

1	0.002	−0.004	−0.0004
−0.49	1	0.009	0.004
−0.6	−0.55	1	0.016
0.006	−0.55	0.0006	1

A comparison of its non-diagonal coefficients with those of the matrix $\hat{G}$ demonstrates their correspondence: the values of the «zero» coefficients of the coupling matrix correspond to the values of the matrix $\hat{S}$ on the order of one percent or less, and the remaining coefficients are in the vicinity of 0.5. The averages from S_{ij} calculated using the same set of values are shown in Table 2. A comparison of both tables indicates their similarity. Therefore, to estimate connectivity, one can use either of the two methods of statistical processing of the results, either by calculating probability densities or simply by calculating averages. The spread of the obtained influence coefficients can be estimated by the values of their standard deviations σ_{ij}. The latter are also given for non-diagonal elements in Table 2.

Table 2. The average values of the coefficients of matrix $\hat{S}$ and their standard deviations

1	-0.004 ± 0.04	-0.004 ± 0.015	-0.0002 ± 0.007
-0.47 ± 0.15	1	0.002 ± 0.03	0.009 ± 0.01
-0.53 ± 0.13	-0.52 ± 0.1	1	0.011 ± 0.02
0.015 ± 0.07	-0.52 ± 0.12	-0.002 ± 0.02	1

4. Measuring connectivity under noise conditions

The results obtained in Section (3) refer to a purely deterministic system with chaotic dynamics. How much will they change in the presence of noise that distorts the signals of subsystems? This issue is fundamentally important for using the algorithm in practice, since it is usually difficult to separate signals from noise. In work [2], the influence of internal noise (that is, that created by the ensemble subsystems themselves) was considered and it was shown that it almost does not interfere with the diagnosis of ensemble connectivity using ANN. Here we will consider the influence of external noise, which is generated by third-party sources and added to the generated signals, masking them from the neural network.

Let us calculate S_{ij} with the same parameters as in the previous sections, but we will use «noisy» variables as the observed data: $u_i(n) = x_i(n) + \nu_i \xi_i(n)$, where ξ_i are sources of white Gaussian noise of unit dispersion, ν_i is their intensity. Next, we will consider the same sources: $\nu_i = \nu$ for all i. The variables u_i are used in calculations in equal way as x_i were previously used x_i.

Let us use the same technique to determine the coupling coefficients as in the previous section, gradually increasing the noise intensity from $\nu = 0$ to $\nu = 0.05$. We will track the values of the standard deviations σ_{12} and σ_{21}, the mean squared error of the training Φ, as well as $|\langle S_{12} \rangle|$ and $|\langle S_{21} \rangle|$. Graphs of the obtained dependencies are shown in Fig. 6, *a* and in Fig. 6, *b*.

To begin with, we pay attention to the effect of masking noise on the ability of ANN to predict the dynamics of an ensemble. As expected (see graph $\Phi(\nu)$ in Fig. 6, *a*), as the noise increases, the network's predictive ability deteriorates. However, up to $\nu \simeq 0.001$ the average error of prediction remains small, showing rapid growth only after $\nu \simeq 0.002$.

The deterioration of the performance of the ANN as a predictor filter also affects the ability to recognise the connectivity of an ensemble, which is expressed both in a deterioration in the predictability of the calculated influence coefficients and in a shift in their average values. The analysis of the dependencies of the standard deviations shows (see Fig. 6, *a*), that the latter remain small up to $\nu = 0.005$, demonstrating rapid growth after $\nu \simeq 0.01$. As for the averages themselves, the value of the nonzero coefficients, taken modulo, remains approximately the same as in the absence of noise. However, the same cannot be said about zero coefficients. As follows from Fig. 6, *b*, on the contrary, there is a monotonous increase with

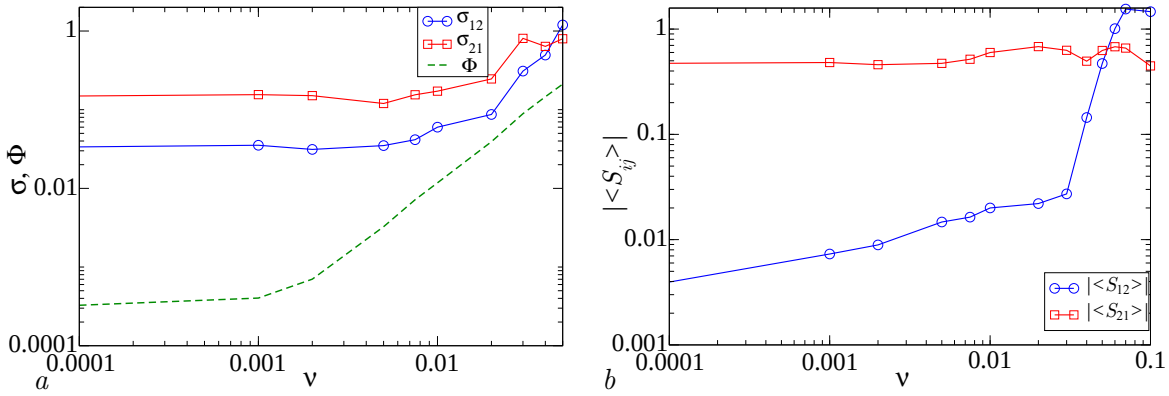

Fig. 6. Dependence of the standard deviations (a) and the modulus of averages (b) for the coefficients S_{12} and S_{21} on the intensity of the external noise ν; the dashed line in figure a plots graph $\Phi(\nu)$

increasing noise intensity. At the same time, up to $\nu \simeq 0.02$, the growth rate is almost constant and remains relatively small, and at $\nu > 0.02$, a rapid increase is observed to values comparable to $|\langle S_{21}\rangle|$. As a result, up to $\nu \simeq 0.002$ the value of $|\langle S_{12}\rangle|$ remains within one percent, and at $0.002 < \nu < 0.02$ it remains within several percent.

Thus, as expected, masking external noise degrades the algorithm's performance. For the system under consideration, the algorithm can be assumed to work reliably up to $\nu \simeq 0.002$ and work up to $\nu \simeq 0.02$; with more noise, it can no longer be used. Since the standard deviation for the signals generated by the maps themselves is $\sigma_x \simeq 0.2$, then the maximum allowable level of external noise is a tenth, and satisfactory is a hundredth of the magnitude of the signal.

Conclusion

The article discusses a method for identifying the structure of couplings in a network of non-identical chaotic maps using ANN. It is a modification of the algorithm proposed in [1] and is based on the training of direct propagation ANN using the regularization procedure. Unlike the previous version, the new algorithm allows to determine the structure of the couplings of the entire ensemble as a whole instead of sequentially identifying the couplings of each of the maps separately.

Studies have shown that the method works effectively for non-identical one-dimensional chaotic systems with linear couplings and an arbitrarily chosen topology. Presumably, it should operate also for multidimensional systems with nonlinear couplings, however, this issue requires additional consideration.

Since the proposed method is based on stochastic ANN training, its results are probabilistic in nature, so that the coupling coefficients obtained from each individual training attempt may differ from each other. Nevertheless, the calculated coefficients of «inactive» couplings always remain significantly lower than «active» and are, as a rule, on the order of one percent. Statistical processing should be used to improve the reliability of the results. The latter consists of both calculating the ensemble averages of the resulting values and calculating the maximum values of the distribution functions. Both approaches produce similar results.

Studies of connectivity measurement under conditions of external additive white Gaussian noise have shown that the results significantly depend on its intensity. Weak noise ($SNR > 40$ dB) practically does not effect on the reliability of coupling detection. Noise of medium intensity, up to $SNR \sim 20$ dB, worsens the reliability of the prediction, but still allows you to distinguish active couplings from inactive ones. At $SNR < 14$ dB, the differences between the couplings are vanished, and the method completely loses its functionality.

References

1. Shabunin AV. Searching the structure of couplings in a chaotic maps ensemble by means of neural networks. Izvestiya VUZ. Applied Nonlinear Dynamics. 2024;32(5):636–653

(in Russian). DOI: 10.18500/0869-6632-003111.
2. Shabunin AV. Determining the structure of couplings in chaotic and stochastic systems using a neural network. Izvestiya of Saratov University. Physics. 2025;25(3):277–287 (in Russian). DOI: 10.18500/1817-3020-2025-25-3-277-287.
3. Granger CWJ. Investigating causal relations by econometric models and cross- spectral methods. In: Ghysels E, Swanson NR, Watson MW, edirors. Essays in Econometrics: Collected Papers of Clive W. J. Granger. Econometric Society Monographs. Cambridge: Cambridge University Press; 2001. P. 31–47. DOI: 10.1017/CBO9780511753978.002.
4. Granger CWJ. Testing for causality. A personal viewpoint. J. Economic Dynamics and Control. 1980;2:329–352. DOI: 10.1016/0165-1889(80)90069-X.
5. Sysoev IV. Diagnostics of Connectivity by Chaotic Signals of Nonlinear Systems: Solving Reverse Problems. Saratov: Kubik; 2019. 46 p. (in Russian).
6. Hesse R, Molle E, Arnold M, Schack B. The use of time-variant EEG Granger causality for inspecting directed interdependencies of neural assemblies. Journal of Neuroscience Methods. 2003; 124(1):27–44. DOI: 10.1016/S0165-0270(02)00366-7.
7. Bezruchko BP, Ponomarenko VI, Prohorov MD, Smirnov DA, Tass PA. Modeling nonlinear oscillatory systems and diagnostics of coupling between them using chaotic time series analysis: applications in neurophysiology. Phys. Usp. 2008;51:304-–310. DOI: 10.1070/PU2008v051n03ABEH006494.
8. Mokhov II, Smirnov DA. Diagnostics of a cause-effect relation between solar activity and the Earth's global surface temperature. Izv. Atmos. Ocean. Phys. 2008;44:263–272. DOI: 10.1134/S0001433808030018.
9. Mokhov II, Smirnov DA. Empirical estimates of the influence of natural and anthropogenic factors on the global surface temperature. Dokl. Earth Sci. 2009;427:798–803. DOI: 10.1134/S1028334X09050201.
10. Sysoev IV, Karavaev AS, Nakonechny PI. Role of model nonlinearity for Granger causality based coupling estimation for pathological tremor. Izvestiya VUZ. Applied Nonlinear Dynamics. 2010;18(4):81–90. DOI: 10.18500/0869-6632-2010-18-4-81-90.
11. Sysoeva MV, Sysoev IV. Mathematical modeling of encephalogram dynamics during epileptic seizure. Tech. Phys. Lett. 2012;38(2):151–154. DOI: 10.1134/S1063785012020137.
12. Sysoev IV, Sysoeva MV. Detecting changes in coupling with Granger causality method from time series with fast transient processes. Physica D. 2015;309:9–19. DOI: 10.1016/j.physd.2015.07.005.
13. Chen Y, Rangarajan G, Feng J, Ding M. Analyzing multiple nonlinear time series with extended Granger causality. Phys. Lett. A. 2004;324(1):26–35. DOI: 10.1016/j.physleta.2004.02.032.
14. Marinazzo D, Pellicoro M, Stramaglia S. Nonlinear parametric model for Granger causality of time series. Phys. Rev. E. 2006;73(6):066216. DOI: 10.1103/PhysRevE.73.066216.
15. Kornilov MV, Sysoev IV. Recovering the architecture of links in a chain of three unidirectionally coupled systems using the Granger-Causality Test. Tech. Phys. Lett. 2018;44:445–449. DOI: 10.1134/S1063785018050206.
16. Haykin S. Neural Networks. New Jersey: Prentice Hall; 2006. 842 p.
17. Galushkin AI. Neural Networks. The Theory Basics. M.: Telekom; 2012. 496 p. (in Russian).
18. Kulkarni DR, Parikh JC, Pandya AS. Dynamic predictions from time series data – an artificial neural network approach. International Journal of Modern Physics C. 1997;8(6):1345–1360. DOI: 10.1142/S0129183197001193.
19. de Oliveira KA, Vannucci A, da Silva EC. Using artificial neural networks to forecast chaotic time series. Physica A. 2000;284(1–4):393–404. DOI: 10.1016/S0378-4371(00)00215-6.
20. Antipov OI, Neganov VA. Neural network prediction and fractal analysis of the chaotic processes in discrete nonlinear systems. Dokl. Phys. 2011;56:7–9. DOI: 10.1134/S1028335811010034.
21. Shabunin AV. Neural network as a predictor of discrete map dynamics. Izvestiya VUZ. Applied Nonlinear Dynamics. 2014;22(5):58–72. DOI: 10.18500/0869-6632-2014-22-5-58-72.
22. Tank A, Covert I, Foti N, Shojaie A, Fox E. Neural Granger causality for nonlinear time series.

arXiv:1802.05842. arXiv Preprint; 2018. DOI: 10.48550/arXiv.1802.05842.
23. Tihonov AN. On incorrect linear algebra problems and a stable solution method. Soviet Mathematics Doklady. 1965;163(3):591–594 (in Russian).
24. Kolmogorov AN. On the representation of continuous functions of several variables by superpositions of continuous functions of a smaller number of variables. Soviet Mathematics Doklady. 1956;108:179–182.
25. Arnold VI. On function of three variables. Soviet Mathematics Doklady. 1957;114:679–681.